Article

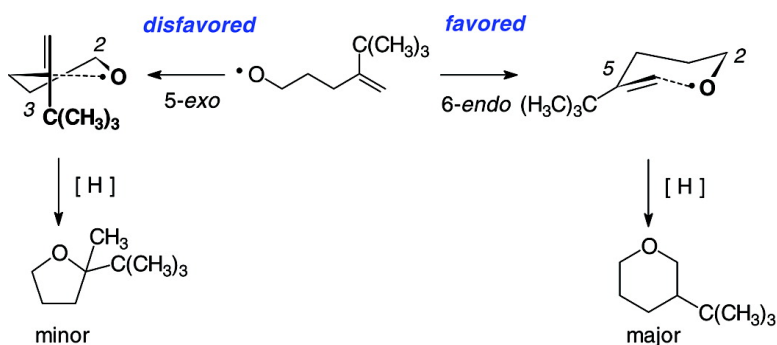# On the 6-*endo* Selectivity in 4-Penten-1-oxyl Radical Cyclizations

Jens Hartung, Rainer Kneuer, Christian Rummey, and Gerhard Bringmann

More About This Article

Additional resources and features associated with this article are available within the HTML version:

- Supporting Information
- Links to the 4 articles that cite this article, as of the time of this article download
- Access to high resolution figures
- Links to articles and content related to this article
- Copyright permission to reproduce figures and/or text from this article

View the Full Text HTML

On the 6-*endo* Selectivity in 4-Penten-1-oxyl Radical Cyclizations

Jens Hartung,*,† Rainer Kneuer, Christian Rummey, and Gerhard Bringmann*

*Contribution from the Institut für Organische Chemie, Universität Würzburg, Am Hubland, D-97074 Würzburg, Germany*

Received February 21, 2004; E-mail: hartung@chemie.uni-kl.de; bringman@chemie.uni-wuerzburg.de

Abstract: Regioselectivities in cyclizations of 4-substituted 4-penten-1-oxyl radicals have been investigated in a combined experimental and computational study (density functional theory). The progressive increase of the 6-*endo*-trig selectivity along the series of 4-substituents H < CH_3 < $C(CH_3)_3$ < C_6H_5 has been interpreted to originate from a balance between strain and FMO interactions. Torsional strain, which is associated with geometrical changes upon an approach of the reacting entities, is relevant for the 6-*endo*-trig but not for the 5-*exo*-trig reactions, as seen, for instance, in selective tetrahydrofuran formation from the 4-penten-1-oxyl radical and its 4-methyl derivative. The preference for tetrahydropyran formation in cyclizations of the 4-*tert*-butyl and the 4-phenyl-4-penten-1-oxyl radical has been attributed to FMO interactions between the terminal carbon atom of the π bond and the *O*-radical center thus favoring the 6-*endo*-trig reaction on the basis of lower transition state energies.

Introduction[1]

The 4-penten-1-oxyl radical (**1a**) cyclizes regioselectively to furnish, after hydrogen atom trapping, a 98:2 mixture of 2-methyltetrahydrofuran (**4a**) and tetrahydropyran (**5a**) ($T = 30$ °C, Scheme 1, $R^2 = H$).[2–4] This fingerprint-type regioselectivity is retained in ring closure reactions of 1-, 2-, and 3-methyl- or phenyl-substituted 4-penten-1-oxyl radicals.[5] A considerable change in this reactivity and selectivity was observed for the 4-phenyl-4-penten-1-oxyl radical (**1d**), which cyclizes at 30 °C approximately 8 times faster via the 6-*endo*-trig pathway than the 4-penten-1-oxyl radical (**1a**) undergoes a 5-*exo*-trig ring closure.[5a]

Scheme 1. Modes of 4-Penten-1-oxyl Radical Cyclizations and Indexing of Compounds **1**−**5**
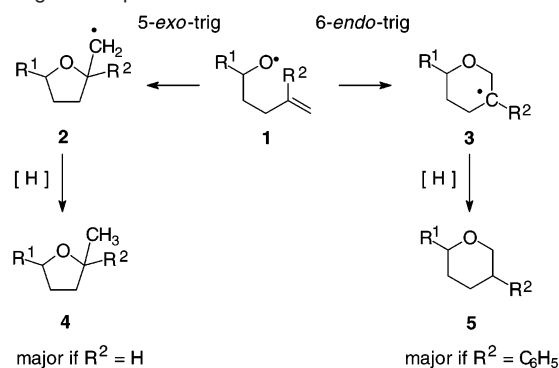
1–5	R^1	R^2
a	H	H
b	H	CH_3
c	H	$C(CH_3)_3$
d	H	C_6H_5
e	CH_3	H
f	CH_3	CH_3
g	CH_3	$C(CH_3)_3$

The 5-*exo*-trig cyclization of alkenoxyl radicals is a transformation of notable synthetic utility.[6] It provides, for example, regioselectivities in a radical version of the halocyclization, which are not attainable from traditional electrophile-induced alkenol cyclizations.[7–9] In view of this mechanistic and synthetic

† Current address: Fachbereich Chemie, Organische Chemie, Technische Universität Kaiserslautern, Erwin-Schrödinger-Strasse, D-67663 Kaiserslautern, Germany.

(1) The following abbreviations have been applied: C = chair conformer (for tetrahydropyran-derived structures); DTA = differential thermoanalysis; E = envelope conformer (for tetrahydrofuran-derived structures); T = twist conformer (for tetrahydrofuran-derived structures); TB = twist boat conformer (for tetrahydropyran-derived structures); ZPVE = zero-point vibrational energy.

(2) For the discovery of the 5-*exo*-trig-cyclization of **1a**, see: (a) Surzur, J.-M.; Bertrand, M.-P.; Nougier, R. *Tetrahedron Lett.* **1969**, 4197−4200. For early work on the 5-*exo*-trig cyclization **1a**→**2a**, see: (b) Rieke, R. D.; Moore, N. A. *J. Org. Chem.* **1972**, *37*, 413−418. (c) Gilbert, B. C.; Holmes, R. G. G.; Laue, H. A. H.; Normann, R. O. C. *J. Chem. Soc., Perkin Trans. 2* **1976**, 1047−1052. (d) Beckwith, A. L. J.; Hay, B. P. *J. Am. Chem. Soc.* **1988**, *110*, 4415−4416. (e) Beckwith, A. L. J.; Hay, B. P.; Williamson, G. M. *J. Chem. Soc., Chem. Commun.* **1989**, 1202−1203.

(3) For the discovery of the 6-*endo*-trig-mode of cyclization of the 4-penten-1-oxyl radical (**1a**) see: Hartung, J.; Gallou, F. *J. Org. Chem.* **1995**, *60*, 6706−6716.

(4) For reviews on the 4-penten-1-oxyl radical cyclization, see: (a) Hartung, J. *Eur. J. Org. Chem.* **2001**, 619−632. (b) Hartung, J. In *Radicals in Organic Synthesis*; Renaud, P., Sibi, M. P., Eds.; Wiley-VCH: Weinheim, 2001; Vol. 2, pp 425−439.

(5) (a) Hartung, J.; Hiller, M.; Schmidt, P. *Chem.−Eur. J.* **1996**, *2*, 1014−1023. (b) Hartung, J.; Hiller, M.; Schmidt, P. *Liebigs Ann. Chem.* **1996**, 1425−1436. (c) Hartung, J.; Schwarz, M.; Svoboda, I.; Fuess, H. *Eur. J. Org. Chem.* **1999**, 1275−1290.

(6) Hartung, J.; Gottwald, T.; Špehar, K. *Synthesis* **2002**, 1469−1498.

(7) (a) Hartung, J.; Kneuer, R.; Laug, S.; Schmidt, P.; Špehar, K.; Svoboda, I.; Fuess, H. *Eur. J. Org. Chem.* **2003**, 4033−4052. (b) Hartung, J.; Kopf, T. M.; Kneuer, R.; Schmidt, P. C. R. *Acad. Sci. Paris, Chemie/Chemistry* **2001**, 649−666. (c) Hartung, J.; Kneuer, R. *Eur. J. Org. Chem.* **2000**, 1677−1683.

Table 1. Preparation of
N-(Alkenoxy)-4-(*p*-chlorophenyl)thiazolethiones **9**

	6	(R = C₄H₉)	8		9
	7	(R = C₂H₅)		CP = *p*-ClC₆H₄	

entry	6,7	8	R¹	R²	9	yield [%]
1	**6**	**8b**	H	CH₃	**9b**	67
2	**6**	**8c**	H	C(CH₃)₃	**9c**	71
3	**7**	**8g**	CH₃	C(CH₃)₃	**9g**	64

background it was the aim of the present study,[10] to uncover in a combined experimental and computational investigation principles that favor 6-*endo*-trig-selective alkenoxyl radical cyclizations. The results of this investigation will contribute to the development of syntheses of tetrahydropyran-derived target compounds in future applications of this hitherto largely unexplored reaction.

Results

1. Preparation and Photochemical Conversion of Alkoxyl Radical Precursors. *N*-(4-Methyl-4-penten-1-oxy)-4-(*p*-chlorophenyl)thiazole-2(3*H*)thione (**9b**) was prepared in 67% yield from the reaction of *N*-(hydroxy)-4-(*p*-chlorophenyl)thiazole-2(3*H*)-thione tetrabutylammonium salt (**6**)[11] and 4-methyl-4-penten-1-yl tosylate (**8b**)[12] in anhydrous DMF (Table 1). Treatment of ammonium salt **6** and 4-(*tert*-butyl)-4-penten-1-yl tosylate **8c**[13] afforded *N*-[4-(*tert*-butyl)-4-penten-1-oxy]thiazolethione **9c** in 71% yield. *N*-[5-(*tert*-Butyl)-5-hexen-2-oxy]-4-(*p*-chlorophenyl)thiazolethione **9g** was prepared from the corresponding tosylate **8g** and tetraethylammonium salt **7** in 64% yield. All thiazolethiones **9** were obtained as colorless and crystalline air stable materials that were stored in standard glassware in a refrigerator.

N-(4-Methyl-4-penten-1-oxy)thiazolethione **9b** and [(H₃C)₃-Si]₃SiH (2.2 equiv, c_o = 0.18 M) were dissolved in deaerated C₆D₆. Photolysis of this solution at 20 °C was performed in a Rayonet chamber photoreactor equipped with λ = 350 nm light bulbs (Supporting Information). The starting material **9b** was consumed within 25 min to provide 56% of 2,2-(dimethyl)-tetrahydrofuran (**4b**)[14] and 25% of 3-methyltetrahydropyran (**5b**) (¹H NMR, Table 2). 4-Methyl-4-penten-1-ol, i.e., the product of direct hydrogen atom trapping of *O*-radical **1b**, was not

(8) Hartung, J.; Kneuer, R. *Tetrahedron: Asymmetry* **2003**, *14*, 3019−3031.
(9) (a) Hartung, J.; Greb, M. *Tetrahedron Lett.* **2003**, *44*, 6091−6063. (b) Jung, M. E.; Fahr, B. T.; D'Amico, D. C. *J. Org. Chem.* **1998**, *63*, 2982−2987. (c) Corey, E. J.; Ha, D.-C. *Tetrahedron Lett.* **1988**, *29*, 3171−3174. (d) González, A. G.; Martín, J. D.; Pérez, C.; Ramírez, M. A.; Ravelo, F. *Tetrahedron Lett.* **1981**, *22*, 5071−5072. (e) Harmange, J.-C.; Figadère, B. *Tetrahedron: Asymmetry* **1993**, *4*, 1711−1754. (f) Bartlett, P. A. In *Asymmetric Synthesis*; Morrision, J. D., Ed.; Academic Press: New York, 1984; Vol. 3, pp 411−453.
(10) Hartung, J.; Stowasser, R.; Vitt, D.; Bringmann, G. *Angew. Chem.* **1996**, *108*, 3056−3059; *Angew. Chem., Int. Ed. Engl.* **1996**, *35*, 2820−2823.
(11) (a) Hartung, J. In *Encyclopedia for Reagents in Organic Synthesis*; Crich, D., Ed.; John Wiley & Sons: New York, NY, in press. (b) Hartung, J.; Schwarz, M. *Org. Synth.* **2002**, *79*, 228−235.
(12) (a) Ansell, M. F.; Thomas, D. A. *J. Chem. Soc.* **1961**, 539−542. (b) Larock, R. C.; Yang, H.; Weinreb, S. M.; Herr, R. J. *J. Org. Chem.* **1994**, *59*, 4172−4178.
(13) Matlin, A. R.; Clifford, C. F.; Wolff, S.; Agosta, W. C. *J. Am. Chem. Soc.* **1986**, *108*, 3385−3394.
(14) Eliel, E. L.; Hargrave, K. D.; Pietrusiewicz, K. M.; Manoharan, M. *J. Am. Chem. Soc.* **1982**, *104*, 3635−3643.

Table 2. Synthesis of Tetrahydrofurans **4** and Tetrahydropyrans **5** from *N*-(Alkenoxy)Thiazolethiones **9**[a]

				yield [%]	
entry	1, 4, 5, 9	R¹	R²	X–Y	4	5
1[b]	**b**	H	CH₃	**H** Si(Si(CH₃)₃)₃	56	25
2[b]	**c**	H	C(CH₃)₃	**H** Si(Si(CH₃)₃)₃	34	40
3[c]	**g**	CH₃	C(CH₃)₃	**H** Sn(C₄H₉)₃	18	31

[a] CP = *p*-ClC₆H₄. **10**: Y = [Si(Si(CH₃)₃]₃. **11**: Y = Sn(C₄H₉)₃. [b] Photoreaction in C₆D₆; yields were determined by ¹H NMR using anisole as internal standard (estimated error: ±5%). [c] Photoreaction in C₆H₆; **4g** (cis/trans = 50:50) and **5g** (cis/trans = 13:87) were purified by column chromatography. The ratio of purified **4g** versus **5g** was identical to the value determined by GC from the reaction mixture (quantitative GC analysis: *n*-C₁₄H₃₀ as internal standard; estimated errors for cis/trans and **4g:5g** ratios: ±2%).

detected in the reaction mixture (¹H NMR). The structural formula of 2-[tris(trimethylsilyl)]silylsulfanyl-4-(*p*-chlorophenyl)thiazole (**10**) has been disclosed in the graphics on the basis of its close analogy to the familiar tributyltin-derivative **11** (Table 2).[5c]

Photolysis of *N*-[4-(*tert*-butyl)-4-penten-1-oxy]thiazolethione **9c** in the presence of [(H₃C)₃Si]₃SiH (2.2 equiv, c_o = 0.18 M) in C₆D₆ afforded 34% of 2-methyl-2-(*tert*-butyl)tetrahydrofuran **4c**, 40% of 3-(*tert*-butyl)tetrahydropyran **5c**, and traces of 4-(*tert*-butyl)-4-penten-1-ol (¹H NMR, Supporting Information).[15] Irradiation of a solution of *N*-[5-(*tert*-butyl)-5-hexen-2-oxy]-4-(*p*-chlorophenyl)thiazole-2(3*H*)-thione (**9g**) and (H₉C₄)₃SnH in C₆H₆ furnished, after purification of the reaction mixture by chromatography, 18% of 2,5-dimethyl-2-(*tert*-butyl)tetrahydrofuran **4g** (cis/trans = 50:50) and 31% of 2-methyl-5-(*tert*-butyl)-tetrahydropyran (**5g**) (cis/trans = 13:87). This workup process was monitored by GC in order to verify that the ratio of cyclic ethers **4** and **5** reported in Table 2 corresponds to the information that was present in the original reaction mixture.

2. Computational Studies on the Regioselectivity in Cyclizations of 4-Substituted 4-Penten-1-oxyl Radicals. The energetically most favorable conformer of alkoxyl radicals **1a**−**d**, cyclized radicals **2a**−**d** and **3a**−**d**, and relevant transition structures in 4-penten-1-oxyl radical cyclizations (Table 4) were computed on a density functional (DF) level of theory using the 6-31+G* split valence basis set.[16,17] The data from previous investigations had shown that diffuse *and* polarization wave functions are necessary in order to satisfactorily reproduce the experimentally observed 5-*exo*/6-*endo*-selectivity in ring closure

(15) Mihailovic, M. L.; Gojkovic, S.; Milosavljevic, S.; Konstantinovic, S. *Indian J. Chem.* **1999**, *38B*, 101−105.

Table 3. Synopsis of Selectivities from 4-Penten-1-oxyl Radical Cyclizations in the Presence of Reactive Hydrogen Atom Donors **H**−**Y**[a]

entry	1	R[1]	R[2]	4:5
1	**a**	H	H	98:2[a]
2	**b**	H	CH$_3$	69:31[b]
3	**c**	H	C(CH$_3$)$_3$	46:54[b]
4	**d**	H	C$_6$H$_5$	7:93[a]
5	**e**	CH$_3$	H	98:2[a]
6	**f**	CH$_3$	CH$_3$	82:18[a]
7	**g**	CH$_3$	C(CH$_3$)$_3$	37:63[b]

[a] **H**−**Y** = **H**−Sn(C$_4$H$_9$)$_3$ or **H**−Si[Si(CH$_3$)]$_3$. Reaction temperature: 30 °C; see ref 5. [b] Reaction temperature: 20 °C.

reactions of the 4-penten-1-oxyl radical (**1a**).[10,18] According to information from an assessment of methods that provide reliable relative heats of formation in radical additions to C,C double bonds,[19,20] we restricted ourselves to the use of Becke's three parameter hybrid functional[21,22] for calculations that are outlined below.

Selectivities from kinetically controlled reactions, for instance from cyclizations of *O*-radicals **1** under the conditions applied above,[5,18] may be analyzed by transition state theory, i.e., by taking a Boltzmann distribution of thermal, rotational, and vibrational energies in addition to the computed electronic energies of a complete ensemble of transition states into account.[23] To keep computational time at a reasonable level without losing essential information, simplifications have been made in the present study. The ensemble of transition states was reduced to two energetically lowest transition structures per mode of ring closure (Scheme 2), which simplified the Boltzmann statistics considerably. An assessment of this approach is outlined in the Discussion (see below).

The absence of imaginary harmonic frequencies pointed to minimum structures for radicals **1**−**3** on the corresponding

potential energy surfaces. The computed energies (E + ZPVE), zero-point vibrational energies (ZPVE), expectation values of the spin operator ($\langle S^2 \rangle$), and relative heats of formation ($\Delta \Delta H_f$) of radicals **1**−**3** are listed in Table 4. The illustration in Figure 1 has been restricted to phenyl-substituted radicals **1d**−**3d**.[24,25] Differences between the latter and the remaining computed structures [i.e., for R[2] = H, CH$_3$, C(CH$_3$)$_3$] have been included into Table 4.

The search for the two energetically lowest transition structures associated with each mode of ring closure was conducted as follows: A chair- *and* a boatlike folding of the 4-penten-1-oxyl radical **1a** and of its 4-substituted derivatives **1b**−**d** served as input geometries (Scheme 2, center left).[26] A successive shortening of the C4,O (for **12** and **13**) or the C5,O (for **14** and **15**) bond from 3.00 Å to 1.48 Å led to high energy intermediates along the associated reaction coordinates on an AM1 level of theory.[27] The highest energy structure from each linear transit served as input geometry for successfully performing ab initio calculations. Stationary points were located by gradient optimization procedures using the first and second derivatives. The existence of one imaginary harmonic vibrational frequency that was associated with the trajectory of C,O bond formation classified intermediates **12**−**15** as authentic transition structures. The calculated energies (E + ZPVE), zero-point vibrational energies (ZPVE), expectation values of the spin operators ($\langle S^2 \rangle$), relative heats of formation ($\Delta \Delta H_f$, referenced versus the associated alkoxyl radical **1**), sum of electronic and thermal free energies G, ΔG (referenced versus the energetically lowest transition structure of each series of intermediates), Boltzmann-weighted populations P, and a short summary of relevant conformational parameters of transition structures **12a**−**d**, **13a**−**d**, **14a**−**d**, and **15a**−**d** are listed in Tables 5 and 6. For the sake of clarity, the illustration of computed geometries has been restricted to transition structures of cyclizations associated with the 4-phenyl-4-pentenoxyl radical **1d** (Figure 2).

Discussion

1. Experimental Regioselectivities. The 5-*exo*/6-*endo*-selectivity in cyclizations of 4-penten-1-oxyl radicals **1** gradually changes along the series of 4-substituents from 98:2 (**1a**, R[2] = H),[3] via 69:31 (**1b**, R[2] = CH$_3$), 46:54 [**1c**, R[2] = C(CH$_3$)$_3$], to 7:93 (**1d**, R[2] = C$_6$H$_5$)[5a] (Table 3). The product analysis of volatile cyclic ethers **4b**, **5b** (81% combined yield) and **4b**, **5b** (74% combined yield) has been performed directly from the corresponding reaction mixtures (^{1}H NMR, GC). The choice of [(H$_3$C)$_3$Si]$_3$SiH as hydrogen atom donor for this purpose was guided by the observation that ^{1}H NMR resonances originating

(16) Quantum chemical calculations were carried out on Intel LinuX Workstations using the *Gaussian 98* (revision A.7) software: Frisch, M. J.; Trucks, G. W.; Schlegel, H. B.; Scuseria, G. E.; Robb, M. A.; Cheeseman, J. R.; Zakrzewski, V. G.; Montgomery, J. A., Jr.; Stratmann, R. E.; Burant, J. C.; Dapprich, S.; Millam, J. M.; Daniels, A. D.; Kudin, K. N.; Strain, M. C.; Farkas, O.; Tomasi, J.; Barone, V.; Cossi, M.; Cammi, R.; Mennucci, B.; Pomelli, C.; Adamo, C.; Clifford, S.; Ochterski, J.; Petersson, G. A.; Ayala, P. Y.; Cui, Q.; Morokuma, K.; Malick, D. K.; Rabuck, A. D.; Raghavachari, K.; Foresman, J. B.; Cioslowski, J.; Ortiz, J. V.; Baboul, A. G.; Stefanov, B. B.; Liu, G.; Liashenko, A.; Piskorz, P.; Komaromi, I.; Gomperts, R.; Martin, R. L.; Fox, D. J.; Keith, T.; Al-Laham, M. A.; Peng, C. Y.; Nanayakkara, A.; Gonzalez, C.; Challacombe, M.; Gill, P. M. W.; Johnson, B.; Chen, W.; Wong, M. W.; Andres, J. L.; Gonzalez, C.; Head-Gordon, M.; Replogle, E. S.; Pople, J. A. *Gaussian 98,* revision A.7; Gaussian, Inc.: Pittsburgh, PA, 1998.

(17) (a) Ditchfield, R.; Hehre, W. J.; Pople, J. A. *J. Chem. Phys.* **1971**, *54*, 724−728. (b) Hehre, W. J.; Ditchfield, R.; Pople, J. A. *J. Chem. Phys.* **1972**, *56*, 2257−2261. (c) Hariharan, P. C.; Pople, J. A. *Mol. Phys.* **1974**, *27*, 209−214.

(18) Maxwell, B. J.; Smith, B. J.; Tsanaktsidis, J. *J. Chem. Soc., Perkin Trans.* **2000**, 425−431.

(19) (a) Barckholtz, C.; Barckholtz, T. A.; Hadad, C. M. *J. Phys. Chem. A* **2001**, *105*, 140−152. (b) Ricca, A.; Bauschlicher, C. W., Jr. *Chem. Phys. Lett.* **2000**, *328*, 396−402. (c) Alvarez-Idaboy, J. R.; Mora-Diez, N.; Vivier-Bunge, A. *J. Am. Chem. Soc.* **2000**, *122*, 3715−3720. (d) Wong, M. W.; Radom, L. *J. Phys. Chem.* **1995**, *99*, 8582−8588.

(20) (a) Jursic, B. S. *THEOCHEM* **1999**, *492*, 285−291. (b) Van Speybroeck, V.; Borremans, Y.; Van Neck, D.; Waroquier, M.; Wauters, S.; Saeys, M.; Marin, G. B. *J. Phys. Chem. A* **2001**, *105*, 7713−7723. (c) Milet, A.; Arnaud, R. *J. Org. Chem.* **2001**, *66*, 6074−6082.

(21) Becke, A. D. *J. Chem. Phys.* **1993**, *98*, 5648−5652.

(22) Lee, C.; Yang, W.; Parr, R. G. *Phys. Rev.* **1998**, *B37*, 785−789.

(23) Eyring, J. *J. Chem. Phys.* **1935**, *3*, 107−115.

(24) The following notation has been applied for tetrahydrofuran and tetrahydropyran-derived structures: C = chair, E = Envelope, T = twist, TB = twist boat. For reasons of symmetry, the following notations are equivalent: $_2T^3 = {_3}T^2$, ${_3}T^4 = {_4}T^3$, ${^4}C_1 = {^1}C_4$, ${_3}TB^5 = {_5}TB^3$: Lehmann, J. *Kohlenhydrate*; Thieme: Stuttgart, 1996; pp 16−37.

(25) Nomenclature for twist and envelope conformers: superscripts are used for atoms which are displaced above the plane of three (T conformers) or four atoms (E conformer). Subscripts refer to atoms which are located underneath these planes. For a proper assignment of subscripts and superscripts of conformers, the atoms of the heterocyclic core, which define a plane, follow a clockwise arrangement with increasing atom count (i.e., O1−C2−C3): (a) Romers, C.; Altona, C.; Buys, H. R.; Havinga, E. *Top. Stereochem.* **1969**, *4*, 39−97. (b) Zschunke, A. *Molekülstruktur*; Spektrum Akademischer Verlag: Heidelberg, 1993; pp 118−136.

(26) Beckwith, A. L. J.; Schiesser, C. H. *Tetrahedron* **1985**, *41*, 3925−3941.

(27) Dewar, M. J. S.; Zoebisch, E. G.; Healy, E. F.; Stewart, J. J. P. *J. Am. Chem. Soc.* **1985**, *107*, 3902−3909.

Scheme 2. Presentation of the Reaction Model for a Computational Analysis on the Regioselectivity in 4-Penten-1-oxyl Radical Cyclizations (Indexing for Radicals **1**−**3** and Transition Structures **12**−**15**: **a** for R^2 = H, **b** for CH_3, **c** for $C(CH_3)_3$, **d** for C_6H_5)[24,25]
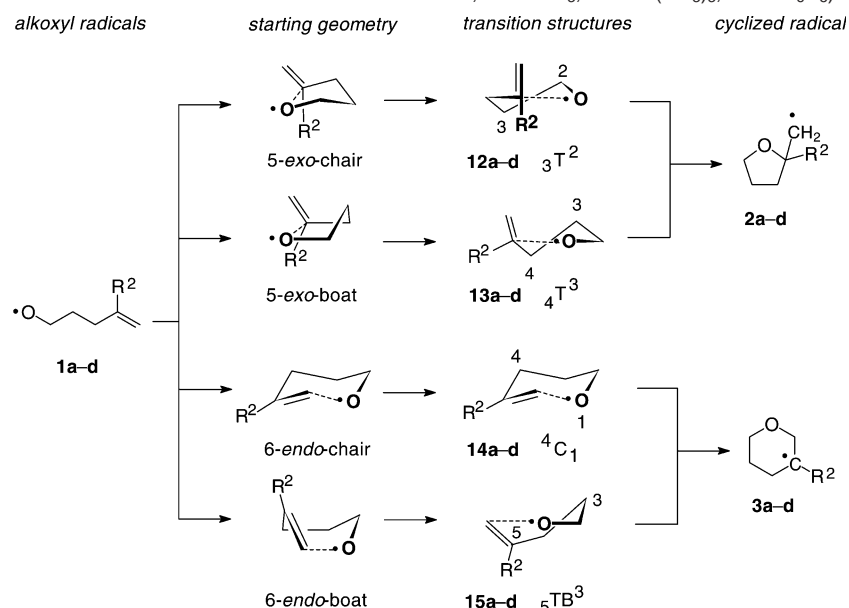

Table 4. Computed Energies (E + ZPVE), Zero-Point Vibrational Energies (ZPVE), $\langle S^2 \rangle$ Values, and Relative Heats of Formation ($\Delta\Delta H_f$) of Radicals **1**−**3**[a]

	parameter	1	2	3
1a → **2a** + **3a**	E + ZPVE[b]	−270.961 894	−270.977 889	−270.981 720
(R^2 = H)	ZPVE[c]	334.091	341.243	345.696
	$\langle S^2 \rangle$	0.754	0.754	0.754
	$\Delta\Delta H_f$[d]	≡ 0	−42.0	−52.1
	conformer[e]	f	$_3T^4$	$^4C_1$
1b → **2b** + **3b**	E + ZPVE[b]	−310.250 355	−310.267 820	−310.275 300
(R^2 = CH_3)	ZPVE[c]	412.089	414.868	419.858
	$\langle S^2 \rangle$	0.754	0.754	0.754
	$\Delta\Delta H_f$[d]	≡0	−45.9	−65.5
	conformer[e]	f	$^2T_3$	$^4C_1$
1c → **2c** + **3c**	E + ZPVE[b]	−428.101 774	−428.120 426	−428.127 387
[R^2 = $C(CH_3)_3$]	ZPVE[c]	632.787	637.533	644.378
	$\langle S^2 \rangle$	0.754	0.754	0.754
	$\Delta\Delta H_f$[d]	≡0	−49.0	−67.2
	conformer[e]	f	$^5T_1$	$^4C_1$
1d → **2d** + **3d**	E + ZPVE[b]	−501.942 909	−501.950 292	−501.976 864
(R^2 = C_6H_5)	ZPVE[c]	548.674	556.882	562.431
	$\langle S^2 \rangle$	0.754	0.754	0.777
	$\Delta\Delta H_f$[d]	≡0	−19.4	−89.1
	conformer[e]	f	$^3T_4$	$^4C_1$

[a] UB3LYP//6-31+G*//UB3LYP/6-31+G*. [b] E (not temperature corrected) + ZPVE in au; 1 au = 2625.50 kJ mol^{-1}. [c] ZPVE in kJ mol^{-1}. [d] $\Delta\Delta H_f$ in kJ mol^{-1} (ZPVE-corrected). [e] For cyclization products **2** and **3**. [f] Open chain conformation; see Figure 1.[1]

from its derived silicon compounds do not interfere with signals belonging to products from alkoxyl radical reactions thus allowing us to determine reliable product ratios. In an additional experiment, 2-methyl-5-(*tert*-butyl)tetrahydropyran **5g** and 2-(*tert*-butyl)-2,5-(dimethyl)tetrahydrofuran **4g** have been prepared from *N*-(alkenoxy)thiazolethione **9g** and Bu$_3$SnH. The formation of tetrahydropyran *trans*-**5g** as major product (**4g**:**5g** = 37:63, 49% combined yield of analytically pure compounds, Supporting Information) from the 6-*endo*-trig reaction of intermediate **1g** and subsequent hydrogen atom transfer onto cyclized radical **3g** is in agreement with the well-known preference of alicyclic six-membered radicals to furnish products of axial trapping in homolytic substitution reactions (Scheme 3).[28] A hydrogen atom delivery from the opposite face gives rise to additional torsional
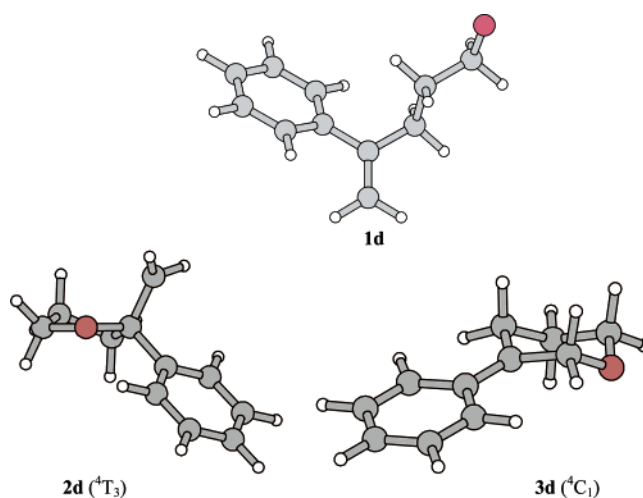
Figure 1. Ball and stick presentation of computed structures for the 4-phenyl-4-penten-1-oxyl radical (**1d**) and cyclization products **2d** and **3d**. Oxygen atoms are depicted in red, carbon atoms, in gray, and hydrogen atoms, in white.[24,25]

strain originating from a transit of the *tert*-butyl substituent past both pseudoequatorially located neighboring hydrogen atoms.[28]

2. Equilibrium Conformations of Alkoxyl Radicals and Cyclized Radicals. The computed geometries of alkoxy radicals **1a**−**d** show the typical alignment of an oxy-functionalized aliphatic chain that is terminated on one side by an olefinic π bond. The 4-phenyl substituent in *O*-radical **1d** is twisted out of a plane that is defined by C4, C5, and the *ipso*-carbon (C$_{ipso}$) (40.25°, Figure 1), unlike the planar structure of α-methylstyrene in the solid state.[29] The heterocyclic core of 5-*exo*-trig cyclization products **2a**−**d** adopts either a $_3T^4$ (in **2a** and **2b**: CH$_2$• substituent located in a pseudoequatorial position) or a $^3T_4$ conformation [in **2c** and **2d**: C(CH$_3$)$_3$ or C$_6$H$_5$ in pseudoequatorial and CH$_2$• in pseudoaxial location; Figure 1, Table 4].[1,24,25]

(28) This interpretation is based on results from an investigation on diastereoselective 4-*tert*-butyl cyclohexyl radical reactions: Damm, W.; Giese, B.; Hartung, J.; Hasskerl, T.; Houk, K. N.; Hüter, O.; Zipse, H. *J. Am. Chem. Soc.* **1992**, *114*, 4067−4079.

(29) Bond, A. D.; Davies, J. E. *Acta Crystallogr.* **2002**, *E58*, o331−o333.

Table 5. Calculated Data, Boltzmann-Weighted Population P and Conformational Details of Transition Structures **12**−**15**[1,24−26 a]

12–15	data	12	13	14	15
a	$E + ZPVE^{b}$	−270.954 669	−270.951 341	−270.951 861	−270.947 240
$R^2 =$ H					
	$ZPVE^{c}$	338.988	338.628	340.895	339.852
	$\langle S^2 \rangle$	0.779	0.779	0.773	0.776
	$\Delta\Delta H_f^{d}$	19.0	27.7	26.3	38.5
	G^{e}	−270.984 621	−270.981 713	−270.981403	−270.977 204
	ΔG^{f}	≡0	7.6	8.4	19.5
	$P\ [\%]^{g}$	92.53	4.31	3.12	0.04
	conf.^{h}	$_2T^3$	$_3T^4$	$^1C_4$	$_5TB^3$
	subst.^{i}	b^{endo}/b^{exo}	pe/pa	j	j
b	$E + ZPVE^{b}$	−310.245 926	−310.243 446	−310.245 422	−310.241 082
$R^2 =$ Me					
	$ZPVE^{c}$	412.214	412.073	414.274	413.588
	$\langle S^2 \rangle$	0.777	0.774	0.770	0.773
	$\Delta\Delta H_f^{d}$	11.6	18.1	13.0	24.3
	G^{e}	−310.277 574	−310.275 498	−310.277 121	−310.273 270
	ΔG^{f}	≡0	5.5	1.2	11.3
	$P\ [\%]^{g}$	57.62	6.27	35.51	0.60
	conf.^{h}	$_2T^3$	$_3T^4$	$^4C_1$	$_5TB^3$
	subst.^{i}	b^{endo}/b^{exo}	pe/pa	j	j
c	$E + ZPVE^{b}$	−428.097 226	−428.095 559	−428.098 425	−428.094 640
$R^2 =$ tBu					
	$ZPVE^{c}$	636.696	636.310	639.339	638.221
	$\langle S^2 \rangle$	0.775	0.774	0.769	0.772
	$\Delta\Delta H_f^{d}$	11.9	16.3	8.8	18.7
	G^{e}	−428.132976	−428.132003	−428.134407	−428.131101
	ΔG^{f}	3.8	6.3	≡ 0	8.7
	$P\ [\%]^{g}$	16.30	5.95	75.50	2.26
	conf.^{h}	$_2T^3$	$_3T^4$	$^4C_1$	$_5TB^3$
	subst.^{i}	b^{endo}/b^{exo}	pe/pa	j	j
d	$E + ZPVE^{b}$	−501.933 851	−501.931 163	−501.937 365	−501.933 842
$R^2 =$ Ph					
	$ZPVE^{c}$	551.986	552.161	554.894	554.440
	$\langle S^2 \rangle$	0.779	0.776	0.770	0.774
	$\Delta\Delta H_f^{d}$	23.8	30.8	14.6	23.8
	G^{e}	−501.970 808	−501.974 096	−501.974 096	−501.971 029
	ΔG^{f}	8.6	16.0	≡0	8.1
	$P\ [\%]^{g}$	2.91	0.15	93.39	3.56
	conf.^{h}	$_2T^3$	$_3T^4$	$^4C_1$	$_5TB^3$
	subst.^{i}	b^{endo}/b^{exo}	pe/pa	j	j

^{a} UB3LYP//6-31+G*//UB3LYP/6-31+G*. ^{b} E (not temperature corrected) + ZPVE in au; 1 au = 2625.50 kJ mol^{-1}. ^{c} ZPVE in kJ mol^{-1}. ^{d} $\Delta\Delta H_f$ values (ZPVE-corrected) in kJ mol^{-1}, referenced versus the associated alkenoxyl radical **1** (Table 4). ^{e} G (298.15) in au. ^{f} ΔG in kJ mol^{-1}, referenced versus the energetically lowest transition structure in each series of intermediates. ^{g} P [%] was calculated according to the to the following equation: $P_a = [(e^{-\Delta G^a/RT})/ (\Sigma_{i=1}^{4} e^{-\Delta Gi/RT})] \times 100$, where P_a denotes the percentrage contribution of a transition structure "a" to the formation of a cyclization product. ^{h} Classification of the transition structure as a distorted tetrahydrofuran conformer (T = twist conformer; E = envelope conformer) or a distorted tetrahydropyran conformer (C = chair conformer, TB = twist-boat conformer).[24,25] ^{i} Arrangement of substituents in tetrahydrofuran-derived transition structures: R²/=CH₂ (b = bisectional, pa = pseudoaxial, pe = pseudoequatorial; the *exo/endo*-notation is referenced to the spatial arrangement of the terminal methylene group toward tetrahydrofuran atom number 3; see also Figure 3). ^{j} Geometry defined by an approximately planar arrangement of atoms C3, C4, C5, and R^2.

The 6-*endo*-trig cyclization products **3** exhibit $^4C_1$ conformations. The flattening at C3 in tetrahydropyranyl radicals **3a**−**d** originates from the propensity of nucleophilic carbon radicals to adopt a planar geometry (Figure 1, Table 4).[30,31]

3. Reaction Enthalpies. DF theory predicts that 5-*exo*-trig cyclizations of 4-penten-1-oxyl radicals **1** are −42 to −49 kJ mol^{-1} exothermic for 4-H, 4-CH₃-, and 4-C(CH₃)₃-substituted intermediates **1a**−**c** (Table 4). The 5-*exo*-trig reaction of the 4-phenyl-4-pentenoxyl radical **1d** is less exothermic (−19 kJ mol^{-1}), since the *O*-radical addition step is associated with a loss of the α-methylstyrene-type stabilization of the olefinic π bond. The reaction enthalpy for 6-*endo*-trig reactions decreases along the series of cyclizations **1a**→**3a** (−52 kJ mol^{-1}) < **1b**→**3b** (−66 kJ mol^{-1}) ≈ **1c**→**3c** (−67 kJ mol^{-1}) < **1d**→**3d** (−89 kJ mol^{-1}). This sequence is considered to reflect the ability of a substituent at C3 to stabilize heterocyclic radicals **3b**−**d** via either hyperconjugation (**3b**, **3c**) or mesomeric interactions (**3d**).[31]

(30) Leffler, J. E. *An Introduction to Free Radicals*; Wiley: New York, 1993.
(31) Beckwith, A. L. J.; Moad, G. *J. Chem. Soc., Chem. Commun.* **1974**, 472−473.

4. Transition Structures, Activation Enthalpies, and Regioselectivities. Regioselectivities in alkenoxyl radical ring closure reactions have been deduced from a Boltzmann-weighted population of the intermediates **12**−**15**, which has in turn been determined on the basis of ab initio computed ΔG (298.15) values. To perform this analysis, simplifications have been made that relate to temperature effects and the correlation between data from the experiment with those from theory:

(i) Temperature effects: The effect of the reaction temperature in the range of 20−80 °C on regioselectivities in alkenoxyl radical cyclizations is in most instances smaller than the experimental precision for elucidating such product distributions.[3,5a,31,32] Therefore, calculated selectivities at 25 ° were compared to experimental data that refer reaction temperatures of 20 °C (for cyclizations of **1b**, **1c**, **1g**) or 30 °C (for cyclizations **1a**, **1d**−**f**).

(ii) Correlation between theory and experiment: Trapping of structurally simple primary, secondary, and tertiary alkyl radicals with either (H₉C₄)₃SnH or [(H₃C)₃Si]₃SiH proceeds with

(32) Gottwald, T.; Greb, M.; Hartung, J. *Synlett* **2004**, 65−68.

Table 6. Geometrical Parameters for Description of Transition Structures **12** and **13** (5-*exo*-Reaction, Left) and **14** and **15** (6-*endo*-Cyclization, Right)[a]

5-*exo*-trig cyclization   6-*endo*-trig-cyclization

12, 13   **14, 15**

12–15	parameter	12	13	14	15
a $R^2 = H$	$r1$ [Å]	2.050	2.086	2.538	2.599
	$r2$ [Å]	2.644	2.654	2.060	2.036
	$r3$ [Å]	1.377	1.373	1.370	1.373
	ϕ [deg]	99.14	98.09	93.26	97.48
	$\delta1$ [deg]	174.14	174.84	165.11	162.95
	$\delta2$ [deg]	162.17	166.18	162.42	165.30
b $R^2 = CH_3$	$r1$ [Å]	2.066	2.105	2.558	2.615
	$r2$ [Å]	2.571	2.583	2.067	2.045
	$r3$ [Å]	1.381	1.377	1.373	1.374
	ϕ [deg]	94.37	93.43	93.91	97.84
	$\delta1$ [deg]	173.94	175.15	165.00	163.00
	$\delta2$ [deg]	161.31	164.15	166.22	168.05
c $R^2 = C(CH_3)_3$	$r1$ [Å]	2.078	2.118	2.578	2.614
	$r2$ [Å]	2.519	2.539	2.086	2.047
	$r3$ [Å]	1.383	1.38	1.373	1.375
	ϕ [deg]	91.14	90.55	94.10	97.69
	$\delta1$ [deg]	173.78	174.49	165.99	163.40
	$\delta2$ [deg]	159.51	161.41	172.27	170.88
d $R^2 = C_6H_5$	$r1$ [Å]	2.013	2.066	2.624	2.659
	$r2$ [Å]	2.574	2.537	2.189	2.134
	$r3$ [Å]	1.392	1.384	1.370	1.371
	ϕ [deg]	95.12	92.53	92.05	96.24
	$\delta1$ [deg]	174.39	173.36	171.19	165.98
	$\delta2$ [deg]	158.57	161.74	171.11	172.27

[a] $r1 = O-C4$; $r2 = O-C5$; $\phi = O-C4-C5$; $\delta1 = C4-C5-H_a-H_b$; $\delta2 = C5-C4-C3-R^2$.

a similar efficiency. Therefore, it is reasonable to directly compare relative yields of heterocycles **4** versus **5** (experiment) to regioselectives for the formation of derived radicals **2** and **3** (theory) (Table 7).[33,34]

(a) Conformational Aspects of Calculated Transition Structures. Two transition structures have been located on the potential energy surface of alkenoxyl radicals **1a–d** for each mode of ring closure. Intermediates **12–15** are considered to represent the most significantly populated transition structures for 5-*exo*- and 6-*endo*-trig cyclization for the following reasons:

(i) If classified as distorted conformers of tetrahydrofuran and tetrahydropyran, intermediates **12–15** represent either low-energy conformers (the twist tetrahydrofuran conformer $_2T^3$ or the twist-boat conformer $_3TB^5$ for tetrahydropyran) or global minima ($_3T^4$ for tetrahydrofuran and the chair conformation $^1C_4$ for tetrahydropyran).[24,25,35–38] The fact that a $_2T^3$ conformer

(33) (a) Hartung, J.; Gottwald, T.; Kneuer, R. *Synlett* **2001**, 749–752. (b) Kneuer, R. Diploma Thesis, Universität Würzburg, 1996.
(34) Chatgilialoglou, C. In *Radicals in Organic Synthesis*; Renaud, P., Sibi, M. P., Eds.; Wiley-VCH: Weinheim, 2001; Vol. 1, pp 28–49.
(35) The atom count changes by +1 in going from a 4-penten-1-oxyl radical (i.e., numbering of carbon atoms) to the corresponding 5-*exo*-trig cyclization product or a tetrahydrofuran-derived transition structure, since the Hantzsch–Widman convention applies for all conformers with a heterocyclic core (i.e., oxygen has a higher priority than carbon).

12d ($_2T^3$)   **13d** ($_3T^4$)

14d ($^4C_1$)   **15d** ($_5TB^3$)

Figure 2. UB3LYP/6-31+G*-optimized geometries of transition structures **12d–15d** for cyclization of the 4-phenyl-4-penten-1-oxyl radical (**1d**) (see also Figure 1). Oxygen atoms are depicted in red, carbon atoms, in gray, and hydrogen atoms, in white.[1,24,25]

Scheme 3. Formation of Tetrahydropyran *trans*-**5g** from 6-*endo*-trig-Cyclized Radical **3g**

3g   **trans**-**5g**

Bu$_3$Sn–H   Bu$_3$Sn•
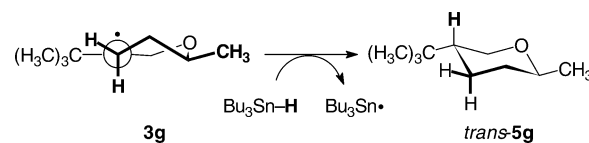
Table 7. Experimental and Calculated Regioselectivities in Cyclizations of 4-Penten-1-oxyl Radicals **1a–d**

entry	1	R^1	R^2	4:5 (experiment)	2:3 (theory)
1	**a**	H	H	98:2[a]	97:3
2	**b**	H	CH_3	69:31[b]	64:36
3	**c**	H	$C(CH_3)_3$	46:54[b]	22:78
4	**d**	H	C_6H_5	7:93[a]	2:97

[a] Reaction temperature 30 °C. [b] Reaction temperature = 20 °C; **H**–Y = **H**–Sn(C_4H_9)$_3$ or **H**–Si[Si(CH_3)$_3$]$_3$.

(Figure 3) is consistently favored over a $_3T^4$ arrangement is

(36) A twist-like transition structure has recently been observed in a 5-*exo*-trig cyclization of an an acetal-derived alkyl radical: Corminboeuf, O.; Renaud, P.; Şchiesser, C. H. *Chem.—Eur. J.* **2003**, *9*, 1578–1584.
(37) (a) Štrajbl, M.; Florián, J. *Theor. Chem. Acc.* **1998**, *99*, 166–170. (b) Han, J. S.; Kang, Y. K. *THEOCHEM* **1996**, *363*, 157–165.
(38) Freeman, F.; Kasner, J. A.; Kasner, M. L.; Hehre, W. J. J. *THEOCHEM* **2000**, *496*, 19–39.

Figure 3. Atom count in alkoxyl radical **1a** and tetrahydrofuran-derived transition structures ($_2$T^3 conformers) **12a** (b^{exo} arrangement of the =CH$_2$ group) and **13a** (b^{endo} positioning of the =CH$_2$ group) for the 5-*exo*-trig mode of cyclization.[35]

thought to originate from a combination of strain and stereo-electronic effects. Thus, the favored path for *O*-radical addition to an olefinic π-bond proceeds along a Bürgi–Dunitz-type trajectory.[39] The computed angle O−C4−C5 = 99.14° (for **1a**, Table 6) is smaller than the expected value of ~120°. The restricted chain length of the alkenoxyl radical causes the approach of the *O*-radical center onto C4 to follow a path that leads to an E^3 arrangement, which relaxes via minor conformational changes into the less strained $_2$T^3-configured intermediate **12**.

(ii) The positioning of substituents in transition structures **12**–**13** for the 5-*exo*-trig mode of cyclization follows the trend that the =CH$_2$ group prefers an *exo*-bisectional position (hereafter b^{exo}), if R^2 = H, CH$_3$ (Figure 3).[40] In the case of R^2 = C(CH$_3$)$_3$, C$_6$H$_5$, the =CH$_2$ group is located in the *endo*-bisectional (hereafter b^{endo}) and the larger substituent in b^{exo} arrangement. The positioning of substituents in transition structures **14**–**15** from the 6-*endo*-trig reactions is governed by a virtually planar configuration of the olefinic subunits at that stage of the reaction.

(b) Activation Enthalpies. The computed activation enthalpies $\Delta\Delta H^{\ddagger}$ for 5-*exo*-trig cyclizations of **1a**–**1c** via $_2$T^3-arranged transition structures **12a**–**c** ($\Delta\Delta H^{\ddagger}$ = 19 kJ mol^{-1} for **1a**, 12 kJ mol^{-1} for **1b** and **1c**) are smaller than the value obtained for the 4-phenyl-4-pentenoxyl radical **1d** ($\Delta\Delta H^{\ddagger}$ = 24 kJ mol^{-1}). The enthalpic barrier is consistently larger for the alternative 5-*exo*-trig pathway that proceeds via $_3$T^4-arranged transition structures **13a**–**d** ($\Delta\Delta H^{\ddagger}$ = 28 kJ mol^{-1} for **1a**, 18 kJ mol^{-1} for **1b**, 16 kJ mol^{-1} for **1c**, 31 kJ mol^{-1} for **1d**). Similar differences were noted for the two 6-*endo*-trig routes. Reactions that proceed via ^{4}C$_1$-arranged intermediates **14a**–**d** ($\Delta\Delta H^{\ddagger}$ = 26 kJ mol^{-1} for **1a**, 13 kJ mol^{-1} for **1b**, 9 kJ mol^{-1} for **1c**, 15 kJ mol^{-1} for **1d**) are characterized by lower activation enthalpies than those which occur via the twist-boat-derived transition structures **15a**–**d** ($\Delta\Delta H^{\ddagger}$ = 39 kJ mol^{-1} for **1a**, 24 kJ mol^{-1} for **1b**, 19 kJ mol^{-1} for **1c**, 24 kJ mol^{-1} for **1d**). A comparison of activation enthalpies from competing reaction channels points to comparatively low barriers for 6-*endo*-trig cyclizations of the 4-(*tert*-butyl)-4-penten-1-oxyl radical **1c** and its 4-phenyl derivative **1d** via ^{4}C$_1$-arranged transition structures **14c** and **14d**. This observation is in agreement with the kinetic effect that favors formation of tetrahydropyran **5d** from intermediate **1d** in the experiment.[5a]

(c) Regioselectivities in Alkenoxyl Radical Ring Closures. The computed regioselectivities point to an increasing preference for formation of the 6-*endo*-trig cyclization product **3** along the series of radicals **1a** (**2a**:**3a** = 97:3), **1b** (**2b**:**3b** = 64:36), **1c** (**2c**:**3c** = 22:78), and **1d** (**2d**:**3d** = 3:97). With one exception

(39) Kirby, A. J. *Stereoelectronic Effects*; Oxford University Press: New York, 1996.

(40) Bogner, J.; Duplan, J.-C.; Infarnet, Y.; Delmut, J.; Huet, J. *Bull. Chim. Soc. Fr.* **1972**, 3616−3624.

Figure 4. Transition structure **16** for the methoxyl radical addition to propene (UB3LYP/6-31+G*//UB3LYP/6-31+G*). ϕ = O−C1−C2 = 103.06°.[44,45]

(entry 3, Table 7), these values agree remarkably well with the ratios of the corresponding cyclic ethers that have been measured experimentally. The correlation of the experimental and the computed regioselectivity for cyclization of 4-(*tert*)-butyl-substituted 4-penten-oxyl radicals **1c** and **1g** (for **1g**: **4**:**5** = 37:63) still is satisfactory, in particular due to the fact that the selected method is able to reproduce the reversal in the 5-*exo*-trig selectivity toward tetrahydropyran formation adequately.

5. Origin of the 6-*endo*-trig Selectivity in Cyclizations of 4-Penten-1-oxyl Radicals. The addition of the methoxyl radical to propene[41] serves as an archetype for alkoxyl radical additions to olefins in general, since no conformational restraints are imposed by a hydrocarbon backbone that links the reacting entities. According to results from UB3LYP/6-31+G* calculations, the *O*-radical approaches the olefin at C1 with its methyl entity oriented into a direction opposite to the (*Z*)-arranged hydrogen H^a (Figure 4, Supporting Information). The sum of Mulliken charges for the H$_3$CO entity in intermediate **16** is −0.16 (likewise +0.16 for the propene subunit), which points to electrophilic properties of the *O*-radical center in the addition reaction. The distance C1,O = 2.078 Å in transition structure **16** is comparable to C,O values obtained for energetically lowest transition structures in alkenoxyl radical cyclizations (e.g., 2.050 Å for **12a**, 2.067 Å for **14d**). The angle O−C1−C2 = 103.06° of *O*-radical attack onto the π bond is consistently larger than that for the investigated cyclizations (e.g., 99.14° for **12a**, 92.05° for **14d**). The *O*-radical approach to the π bond leads to minor geometrical changes, such as orientation of substituents at C2 toward the incoming radical, whereas hydrogen atoms located at C1 move into the opposite direction (δ1 = C2−C1−H^b−H^a = 163.36°, δ2 = C1−C2−CH$_3$−H^c = 175.53°). The magnitude and the signs of torsion angles δ1 and δ2 agree with the corresponding values of energetically favored transition structures in 4-penten-1-oxyl radical cyclizations (e.g., 162.17° and 174.14° for **12a**, 171.19° and 171.11° for **14d**).

The comparison between intermediate **16** and $_2$T^3-configured transition structure **12a** (5-*exo*-trig reaction) and the ^{4}C$_1$-arranged intermediate **14d** (6-*endo*-trig cyclization) indicates that stereo-electronic requirements for the addition reaction are fulfilled in either mode of cyclization. The notable preference for 5-*exo*-trig ring closure of radical **1a** therefore is considered to originate from strain that is imposed by the alkenoxyl chain, when adopting the energetically disfavored transition structure **14a** (6-*endo*-trig pathway). Parts of these unfavorable contributions arise from a minor but significant structural change that occurs within the olefinic subunit during the *O*-radical encounter. In

(41) Houk, K. N.; Paddon-Row, M. N.; Spellmeyer, D. C.; Rondan, N. G.; Nagase, S. *J. Org. Chem.* **1986**, *51*, 2874−2879.

an early phase of the addition, $R^2 = H$ moves toward the oxygen atom, where it is still located in transition structure **14a** ($\delta 2 = 166.18°$). Upon shortening of the C,O distance and thus formation of the 6-*endo*-trig cyclization product **3a**, the geometry at C4 gradually changes from almost planar with respect to C5, R^2, H^a, H^b to approximately planar with respect to C3,C5, R^2 (for **3d** see Figure 2). This structural change requires a transit of R^2 past H^a and the proximate hydrogen atom at C3, which gives rise to van der Waals repulsions. Similar steric interactions are not present in intermediates **12** and **13** thus providing an interpretation for the preferred 5-*exo*-trig cyclization of 4-pentenoxyl radicals **1a** ($R^2 = H$) and **1b** ($R^2 = CH_3$).

The fact that alkoxyl radicals **1c** [$R^2 = C(CH_3)_3$] and **1d** ($R^2 = C_6H_5$) prefer the 6-*endo*-trig mode of ring closure requires a free activation enthalpy lowering contribution from R^2, to compensate the unfavorable torsional strain that is imposed by the substituent in transition structures **14** and **15**. Intramolecular *O*-radical additions are fast and strongly exothermic reactions with their transition states located early on a reaction coordinate.[3,42−45] Thus, frontier molecular orbital (FMO) theory may be applied in order to analyze selectivities of the underlying addition reactions.[46] Since *O*-radicals exhibit electrophilic properties in addition reactions (see above),[47] the most significant stabilizing contribution in the C,O bond forming transition state should arise from interactions between the radical center (SOMO) and the HOMO, the π-type orbital in alkenoxyl radicals **1**. An orbital analysis indicates that the SOMO−HOMO energy gap for radicals **1a**−**1d** is similar. A change, however, is seen in the relative size of the HOMO coefficient at C5, which increases relative to C4 along the series of radicals **1a** (+7%), **1b** (+18%), **1c** (+19%) to +47% for the 4-phenyl-4-pentenoxyl radical **1d** (Figure 5). The relative increase of the HOMO coefficient at C5 correlates with the propensity of an alkenoxyl radical to undergo the 6-*endo*-trig cyclization. In view of these arguments, the origin of the 6-*endo*-selectivity in 4-penten-1-oxyl radical cyclizations may be summarized as follows:

(i) Substituents that increase the HOMO coefficient at C5 (i.e., the terminal atom of the π bond) direct 4-penten-1-oxyl cyclizations into the 6-*endo*-trig reaction channel.

(ii) If the coefficients of the two C atoms that describe the olefinic π bond are approximately equal in size, 4-penten-1-oxyl radicals preferentially undergo 5-*exo*-trig ring closures because the competing 6-*endo*-trig reaction is disfavored on the basis of strain effects.

Conclusions

Three major results have been obtained in a combined experimental and computational study (density functional theory) on the 6-*endo*-selectivity in cyclizations of 4-substituted 4-pentenoxyl radicals **1**:

(i) Upon cyclization and subsequent trapping with the reactive hydrogen atom donors $(H_9C_4)_3SnH$ or $[(H_3C)_3Si]_3SiH$, 4-*tert*-
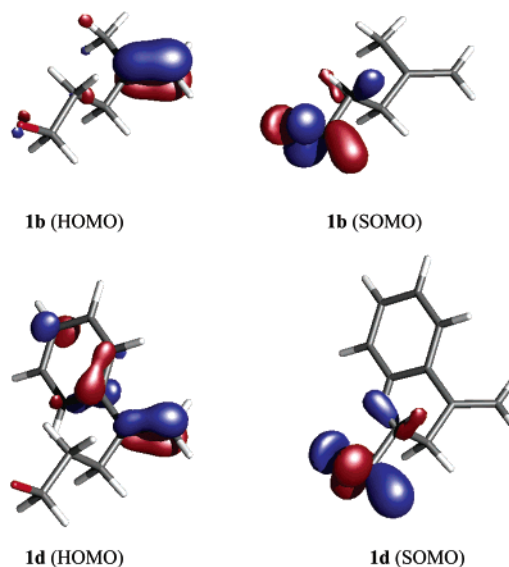
(42) Howard, J. A.; Scaiano, J. C. In *Kinetische Daten von Radikalreaktionen in Lösung − Oxyl, Peroxyl und verwandte Radikale* in *Landolt-Börnstein, Zahlenwerte und Funktionen aus Naturwissenschaft und Technik*, New Series Part D.; Fischer, H., Ed.; Springer: Berlin, 1984; Vol. 13, pp 1−127.
(43) Rothenberg, G.; Sasson, Y. *Tetrahedron* **1998**, *54*, 5417−5422.
(44) Hammond, G. S. *J. Am. Chem. Soc.* **1955**, *77*, 334−338.
(45) (a) Bell, R. P. *Proc. R. Soc. London*, **1936**, *154A*, 414. (b) Evans, M. G.; Polanyi, *Trans. Faraday Soc.* **1938**, *34*, 11.
(46) Fleming, I. *Grenzorbitale und Reaktionen organischer Verbindungen*; Wiley-VCH: Weinheim, 1990.
(47) Jones, M. J.; Moad, G.; Rizzardo, E.; Solomon, D. H. *J. Org. Chem.* **1989**, *54*, 1607−1611.

Figure 5. Presentation of HOMOs (left) and SOMOs (right) of alkoxyl radicals **1b** (top) and **1d** (bottom) (UB3LYP/6-31+G*).

1b (HOMO)   **1b** (SOMO)

1d (HOMO)   **1d** (SOMO)

butyl-substituted 4-penten-1-oxyl radicals **1c** and **1g** furnish tetrahydropyrans **5c** and **5g** as major products.

(ii) Regioselectivities in 4-penten-1-oxyl radical cyclizations, which were calculated from a Boltzmann-weighted population of two energetically lowest and therefore most significantly populated transition structures per mode of ring closure, agree qualitatively *and* quantitatively with the experimental data.

(iii) The propensity of the 4-(*tert*-butyl)-4-pentenoxyl radical **1c** and the 4-phenyl derivative **1d** to undergo 6-*endo*-trig-selective cyclizations has been attributed to favorable FMO interactions between the terminal carbon atom of the π bond and the *O*-radical center thus favoring the 6-*endo*-trig reaction on the basis of lower transition state energies.

Experimental Section

Instrumentation and general remarks have been disclosed previously (see also Supporting Information).[7a]

1. Synthesis of Thiohydroxamic Acid *O*-Esters: General Procedure. A flame-dried round-bottomed flask was charged with anhydrous DMF and an equimolar amount of *N*-hydroxy-4-(*p*-chlorophenyl)-thiazole-2(3*H*)-thione tetraalkylammmonium salt **6** or **7**[11] and alkenyl tosylate **8**. The solution was stirred in an atmosphere of argon for 4−7 d at 20 °C in the dark. Afterward, the reaction mixture was poured into water (40 mL) and extracted with Et_2O (2 × 40 mL). The combined organic phases were washed with 2 N NaOH (30 mL) and dried ($MgSO_4$). The solvent was removed in vacuo to afford a brown oil, which was purified by column chromatography (SiO_2).

***N*-(4-Methyl-4-penten-1-oxy)-4-(*p*-chlorophenyl)thiazole-2(3*H*)-thione (9b).** Thiazolethione **9b** was prepared from 4-methyl-4-penten-1-yl *p*-toluenesulfonate (**8b**)[12] (661 mg, 2.60 mmol) and *N*-hydroxy-4-(*p*-chlorophenyl)thiazole-2(3*H*)-thione tetrabutylammonium salt (**6**) (1.39 g, 2.87 mmol) in anhydrous DMF (3 mL) as described above. The crude product was purified by column chromatography [SiO_2, petroleum ether/Et_2O = 1:1 (v/v)] to afford 570 mg (67%) of thiazolethione **9b** as a colorless solid: mp 68 ± 2 °C (DTA). ^{1}H NMR (250 MHz): $\delta = 1.61$ (s, 3 H, CH_3), 1.71 (m$_c$, 2 H, 2-H), 1.95 (dd, 2 H, $J = 7.0$, 8.2 Hz, 3-H), 4.07 (t, 2 H, $J = 6.7$ Hz, 1-H), 4.51 (s, 1 H, 5-H), 4.64 (s, 1 H, 5-H), 6.51 (s, 1 H, 5′-H), 7.45 (d, 2 H, $J = 8.9$ Hz, ArH), 7.54 (d, 2 H, $J = 8.9$ Hz, ArH). ^{13}C NMR (63 MHz): $\delta = 22.2$, 25.4, 33.3, 76.0, 105.4, 110.3, 126.6, 129.1, 129.6, 136.3, 139.8, 144.1, 180.6. MS (70 eV, EI): m/z (%) = 325 (2) [M$^+$], 227 (18) [C_9H_6-ClNS$_2$], 168 (19) [C_8H_5ClS$^+$], 41 (100) [$C_3H_5^+$]. IR: ν = 3099, 2942,

1487, 1334, 1216, 1162, 1093, 1052, 1018, 976, 932, 890, 835, 761 cm^{-1}. Anal. Calcd for $C_{15}H_{16}ClNOS_2$ (325.89): C, 55.28; H, 4.95; N, 4.30; S, 19.68. Found: C, 55.31; H, 4.72; N, 4.32; S, 19.54.

***N*-[4-(1,1-Dimethyl-1-ethyl)-4-penten-1-oxy]-4-(*p*-chlorophenyl)-thiazole-2(3*H*)thione (9c).** Thiazolethione **9c** was obtained from 4-(2-methyl-2-propyl)-4-penten-1-yl *p*-toluenesulfonate (**8c**)[13] (131 mg, 0.440 mmol) and *N*-hydroxy-4-(*p*-chlorophenyl)thiazole-2(3*H*)-thione tetrabutylammonium salt (**6**) (181 mg, 0.484 mmol) in anhydrous DMF (1 mL) as described above. Purification of the crude product by column chromatography (SiO$_2$, CH$_2$Cl$_2$) afforded 115 mg (71%) of product **9c** as a colorless solid: mp 102−103 °C. ^{1}H NMR (250 MHz): $\delta = 0.99$ (s, 9 H, CH$_3$), 1.67−1.79 (m, 2 H, 2-H), 1.97 (dd, 2 H, $J = 6.4$, 8.9 Hz, 3-H), 4.11 (t, 2 H, $J = 6.4$ Hz, 1-H), 4.51 (s, 1 H, 5-H), 4.80 (s, 1 H, 5-H), 6.55 (s, 1 H, 5′-H), 7.45 (d, 2 H, $J = 8.9$ Hz, ArH), 7.54 (d, 2 H, $J = 8.9$ Hz, ArH). ^{13}C NMR (63 MHz): $\delta = 26.8$, 27.1, 29.2, 36.1, 76.5, 105.4, 106.0, 126.6, 129.1, 129.6, 136.3, 139.9, 156.5, 180.6. IR: $\nu = 3081$, 2967, 1336, 1158, 1092, 1053, 976, 886, 831, 764 cm^{-1}. MS (70 eV, EI): *m/z* (%) = 243 (39) [$C_9H_6ClNOS_2$], 227 (27) [C_9H_6-ClNS$_2$], 168 (27) [$C_8H_5ClS^+$], 83 (87) [$C_6H_{11}^+$], 55 (100) [$C_4H_7^+$]. Anal. Calcd for $C_{18}H_{22}ClNOS_2$ (367.96): C, 58.76; H, 6.03; N, 3.81; S, 17.43. Found: C, 58.29; H, 6.22; N, 3.77; S, 17.37.

***N*-[5-(1,1-Dimethyl-1-ethyl)-5-hexen-2-oxy]-4-(*p*-chlorophenyl)-thiazole-2(3*H*)thione (9g).** Thiazolethione **9g** was prepared from 5-(1,1-dimethyl-1-ethyl)-5-hexen-2-yl *p*-toluenesulfonate (**8g**) (289 mg, 0.931 mmol) and *N*-hydroxy-4-(*p*-chlorophenyl)thiazole-2(3*H*)-thione tetraethylammonium salt (**7**) (386 mg, 1.04 mmol) in anhydrous DMF (3 mL) as described above. Purification of the crude product was achieved by column chromatography [SiO$_2$, petroleum ether/Et$_2$O = 3:1 (v/v)] to afford 226 mg (64%) of thiazolethione **9g** as a colorless solid: mp 56 ± 2 °C (DTA). ^{1}H NMR (250 MHz): $\delta = 0.96$ (d, 3 H, $J = 6.4$ Hz, 1-H), 1.01 (s, 9 H, CH$_3$), 1.35−1.52 (m, 1 H, 3-H), 1.64−1.79 (m, 1 H, 3-H), 2.03 (m$_c$, 2 H, 4-H), 4.49 (s, 1 H, 6-H), 4.80 (s, 1 H, 6-H), 5.05 (m$_c$, 1 H, 2-H), 6.51 (s, 1 H, 5′-H), 7.44 (d, 2 H, $J = 8.9$ Hz, Ar−H), 7.51 (d, 2 H, $J = 8.9$ Hz, Ar−H). ^{13}C NMR (100 MHz): $\delta = 18.0$, 26.3, 29.2, 33.7, 36.1, 82.6, 105.2, 105.9, 127.4, 129.0, 129.9,

135.9, 141.6, 156.9, 181.1. IR: $\nu = 3060$, 2940, 2840, 1610, 1580, 1470, 1390, 1370, 1350, 1300, 1200, 1140 cm^{-1}. MS (70 eV, EI): *m/z* (%) = 243 (1) [$C_9H_5ClNS_2O^+$], 227 (3) [$C_9H_5ClNS_2$], 155 (3) [$C_{10}H_{19}O^+$], 97 (35) [$C_7H_{13}^+$]. Anal. Calcd for $C_{19}H_{24}ClNOS_2$ (381.99): C, 59.74; H, 6.33; N, 3.67; S, 16.79. Found: C, 59.91; H, 6.42; N, 3.65; S, 16.60.

2. Photolysis of *N*-(Alkenoxy)thiazole-2(3*H*)-thiones 9 in the Presence of Reactive Hydrogen Atom Donors (^{1}H NMR Analysis). A Schlenk flask was charged with a solution of *N*-alkenoxy-4-(*p*-chlorophenyl)thiazole-2(3*H*)-thione **9** in C$_6$D$_6$ in the dark. A defined amount of anisole (internal standard) was added, and the flask was sealed with a rubber septum and cooled to liquid-nitrogen temperature. After thorough evacuation (10^{-2} mbar), the flask was flushed with argon. [(H$_3$C)$_3$Si]$_3$SiH (Fluka) was added via a syringe. The reaction mixture was deaerated by means of two freeze−pump−thaw cycles (Ar was used as flushing gas) and was subsequently warmed in a water bath to 20 °C. The colorless solution was photolyzed for 25 min in a Rayonet chamber photoreactor ($\lambda = 350$ nm) and was immediately analyzed by ^{1}H NMR.

Supporting Information Available: Detailed experimental procedure for the synthesis of thiazolethione **9g**, spectral data and characterization of tetrahydrofurans **4** and tetrahydropyrans **5**, atomic coordinates of radicals **1**−**3** and intermediates **12**−**15**, transition structure **16**, and UHF/6-31+G* computed energies and geometrical parameters of radicals **1**−**3** and intermediates **12**−**15** (PDF). This material is available free of charge via the Internet at http://pubs.acs.org.

JA049010G